Temperature Dependence of the Thermal Conductivity and Thermal Diffusivity of Treated Oil-Palm-Fiber-Reinforced Phenolformaldehyde Composites

Kedar Singh,[1] N. S. Saxena,[1] M. S. Sreekala,[2] S. Thomas[3]

[1]*Condensed Matter Physics Laboratory, Department of Physics, University of Rajasthan, Jaipur, 302004, India*
[2]*Rubber Research Institute of India, Kottyam 686009, Kerala, India*
[3]*School of Chemical Science, M. G. University, Kottayam 686560, Kerala, India*

Received 15 March 2002; accepted 11 January 2003

ABSTRACT: The effective thermal conductivity (λ_e) and effective thermal diffusivity (χ_e) of oil-palm-fiber-reinforced treated composites were measured simultaneously with the transient plane source technique from 50 to 110°C. The fibers of the composites were treated with sodium hydroxide alkali, silanol, and acetic acid. The experimental results for the different treated composites showed that there were variations in λ_e and χ_e over this temperature range. However, the maximum values of λ_e and χ_e were observed at 90°C, in the vicinity of the glass-transition temperatures of these composites. An effort was also made to predict the temperature dependence of λ_e and χ_e through the development of an empirical model. The theoretically predicted values of λ_e and χ_e for these composites were in excellent agreement with the experimental results over the entire range of investigated temperatures. Sudden increases in λ_e and χ_e in the glass-transition region of these composites were indicative of the fact that the crosslinking density decreased and was at a minimum at the temperature at which λ_e and χ_e showed their maxima. © 2003 Wiley Periodicals, Inc. J Appl Polym Sci 89: 3458–3463, 2003

Key words: fibers; reinforcements; glass transition; crosslinking; density

INTRODUCTION

Studies of the thermal transport properties of polymeric materials are important because of the crucial role played by these properties in both processing stages and product uses.[1] The matrix resins for composites are used in structural applications[2] and are widely used as industrial materials because of their good heat resistance, electrical insulation, dimensional stability, and flame and chemical resistance.[3–8] Several reports[9–12] have indicated that the incorporation of natural fibers into thermoset matrices improves the mechanical and thermal transport properties of the composites remarkably. The incorporation of oil palm empty fruit bunch (OPEFB) fibers into a phenolformaldehyde (PF) matrix improves the tensile strength, elongation at break, brittle nature, and buckling characteristics considerably.

The chemical treatment of fibers in composites usually changes their physical properties and makes their chemical structure more thermally stable than that of untreated fibers. The thermal conductivity and thermal diffusivity depend on the density, molecular weight, orientation, and other structural features of the materials.[13]

In the last 3 decades, many efforts have been made toward the measurement of the thermal transport properties of liquids,[14,15] loose granular materials,[16,17] nonconducting composite materials,[18,19] composite building materials,[20] conducting materials,[21] and semiconducting chalcogenide glass.[22] Fiber-reinforced PF composites show glass transitions above room temperature. This temperature is important from the viewpoint of their structural changes and, therefore, their use in commercial and scientific applications.

So far, very few efforts have been made to study the effective thermal conductivity (λ_e) and effective thermal diffusivity (χ_e) over a range of temperatures covering the glass-transition region.[23] Such studies offer an opportunity to investigate the effects of structural changes and chemical treatments of composites on λ_e and χ_e. The thermal conductivity and thermal diffusivity of composites treated with alkali, silanol, and acetic acid with a 40 wt % fiber loading have already been studied at room temperature.[24]

In this work, the variations of λ_e and χ_e with the temperature in these composites were studied experimentally from 50 to 110°C, a range covering the glass-transition region. An empirical model for the temperature dependence of λ_e and χ_e of these composites was also developed by means of a least-squares parabola fit to the experimental results. The transient plane

Correspondence to: N. S. Saxena (n_s_saxena@hotmail.com).

Contract grant sponsor: University of Rajasthan.

Journal of Applied Polymer Science, Vol. 89, 3458–3463 (2003)

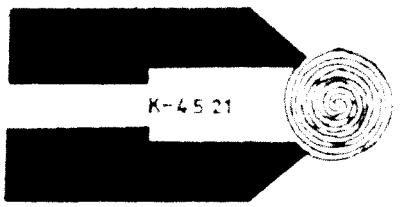

Figure 1 Schematic diagram of the TPS sensor.

source (TPS) method[25] was used for the simultaneous measurement of these properties.

TPS THEORY

The TPS technique has proven to be a precise and convenient method for measuring the thermal transport properties of electrically insulating materials. The TPS method consists of an electrically conducting pattern (Fig. 1) in the form of a bifilar spiral, which also serves as a sensor of the temperature increase in the sample. In Figure 1, K-4521 is the design number of the sensor; K stands for kapton. The sensor is sandwiched between thin insulating layers of kapton. If the conductive pattern is in the Y–Z plane of a coordinate system, the rise in the temperature at a point Y–Z at time t due to an output power per unit of area Q is given by[25]

$$\Delta T(y,z,\tau) = \frac{1}{4\pi^{3/2}a\lambda}\int_0^{\tau}\frac{d\sigma}{\sigma^2}\int_A dy'\,dz' \; Q\left(y'z't-\frac{\sigma^2a^2}{\kappa}\right)\exp\left[\frac{-(y-y')^2-(z-z')^2}{4\sigma^2a^2}\right] \quad (1)$$

where $\chi(t-t')$ is equal to σ^2a^2, θ is equal to a^2/χ, and τ is equal to $(t/\theta)^{1/2}$. a is the radius of the hot disc, which provides a measurement of the overall size of the resistive pattern, and θ is known as the characteristic time. σ is a constant variable, λ is the thermal conductivity (W/m K), and χ is the thermal diffusivity (m^2/s). The temperature increase $\Delta T(y,z,\tau)$, due to the flow of current through the sensor, gives rise to a change in the electrical resistance $\Delta R(t)$:

$$\Delta R(t) = \alpha R_0\,\overline{\Delta T(\tau)} \quad (2)$$

where R_0 is the resistance of the TPS element before the transient recording has been initiated, α is the temperature coefficient of resistance (TCR), and $\overline{\Delta T(\tau)}$ is the properly calculated mean value of the time-dependent temperature increase of the TPS element. During the transient event, $\overline{\Delta T(\tau)}$ can be considered to be a function of time only, whereas, in general, it depends on such parameters as the output power in the TPS element, the design parameters[25] of the resistive pattern, and the thermal conductivity and thermal diffusivity of its surroundings. $\overline{\Delta T(\tau)}$ is calculated by the averaging of the increases in the temperature of the TPS element over the sampling time because the concentric ring sources in the TPS element have different radii and are placed at different temperatures during the transient recording

It is possible to write down an exact solution[25] for the hot disc if it is assumed that the disc contains a number m of concentric rings as sources. From the ring source solution, we immediately get

$$\overline{\Delta T(\tau)} = \frac{P_0}{\pi^{3/2}a\lambda}D_s(\tau) \quad (3)$$

where

$$D_s(\tau) = [m(m+1)]^{-2} \times \int_0^{\tau}\frac{d\sigma}{\sigma^2}\left[\sum_{l=1}^{m} l\left\{\sum_{k=1}^{m} k\exp\frac{-(l^2+k^2)}{4\sigma^2m^2}L_0\left(\frac{lk}{2\sigma^2m^2}\right)\right\}\right] \quad (4)$$

where P_0 is the total output power, L_0 is the modified Bessel function, and l and k are the dimensions of the resistive pattern. For the recording of the potential difference variations, which normally are a few millivolts during the transient recording, a simple bridge arrangement, as shown in Figure 2, is used. If we assume that the resistance increase will cause a potential difference variation $\Delta U(t)$, measured by the voltmeter in the bridge [see Fig. 3 for the $\Delta U(t)$ curve], the analysis of the bridge indicates that

$$\Delta E(t) = \frac{R_s}{R_s+R_0}I_0\Delta R(t) = \frac{R_s}{(R_s+R_0)}\frac{I_0\alpha R_0P_0}{\pi^{3/2}a\lambda}D_s(\tau) \quad (5)$$

where

$$\Delta E(t) = \Delta U(t)[1-C\Delta U(t)]^{-1} \quad (6)$$

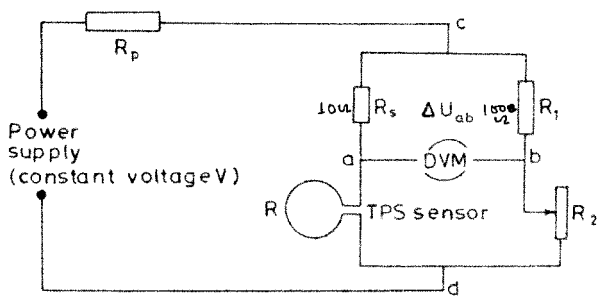

Figure 2 Schematic diagram of the electrical circuit used for the simultaneous measurement of the thermal conductivity, thermal diffusivity, and specific heat per unit of volume.

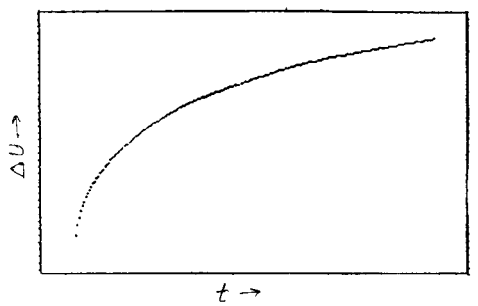

Figure 3 Potential difference ΔU versus time t.

and

$$C = \frac{1}{R_s I_0 \left[1 + \dfrac{\gamma R_p}{\gamma(R_s + R_0) + R_p} \right]} \qquad (7)$$

The definitions of the various resistances are found in Figure 2. R_p is the lead resistance, and R_s is a standard resistance with a current rating that is much higher than I_0, which is the initial heating current through the arm of the bridge containing the TPS element. γ is the ratio of the resistances in the two ratio arms of the bridge circuit and is taken to be 100 in this case.

EXPERIMENTAL

The resole type of PF resin was supplied by West Coast Polymers Pvt., Ltd. (Kannur, India). The solid content of the resin was 50 ± 1%, and caustic soda was used as the catalyst during manufacturing. OPEFBs were obtained from Oil India, Ltd. (Kottayam, India). The OPEFBs were subjected to a retting process, the pithy material was removed, and the fibers were dried. Then, the fibers were cut into fibers 40 mm long, and a randomly oriented mat was prepared. The composites were fabricated by hand lay-up followed by compression molding at 100°C for about 30 min. The volume fraction of the oil palm fibers was 40 wt %. The density of the untreated and treated composites was approximately equal to 1.09 g/cm^3.

Different chemical treatments of the fibers

Alkali treatment

The fibers were dipped into a 5% sodium hydroxide solution for about 48 h. Then fibers were washed separately with water containing a few drops of acetic acid and fresh water and were dried. The OH— groups of the fibers reacted with NaOH as follows:

$$\text{Fiber–OH} + \text{NaOH} \rightarrow \text{Fiber—O—Na}^+ + \text{H}_2\text{O}$$

Acetic acid treatment

The fibers were treated in glacial acetic acid for 1 h and then further treated with acetic anhydride containing concentrated H_2SO_4 as a catalyst for 5 min. The fibers were then washed with water and dried. The reaction took place as follows:

$$\text{Fiber–OH} + \text{CH}_3\text{COOH} \xrightarrow[\text{Conc. } \text{H}_2\text{SO}_4]{(CH_3CO)_2O} \text{Fiber—O—C(=O)—CH}_3 + \text{H}_2\text{SO4}$$

This reaction was expected to take place at the free OH— groups available on cellulose molecules. There was no significant weight change in the fibers on acetylation. The fibers became more hydrophobic after treatment.

Silanol treatment

The fibers were dipped into a 1% silane solution in a water/ethanol mixture (40:60) for about 3 h. The pH of the solution was maintained at 3.5–4.0. The fibers were then washed and dried. The mechanism of bonding between the surface and the silane could be explained as follows.

The alkoxy silanol was able to form bonds with the hydroxyl groups of the cellulose fiber. Silane reacted with water to form silanol and alcohol. Silane further reacted with the OH— group of the fiber surface. This led to a chemical-bond formation between the fiber and the silane. The silanol could, therefore, form polysiloxane structures by a reaction with the hydroxyl groups of the fiber:

$$\underset{\text{(tryethoxy vinyl silane)}}{\text{CH}_2\text{CHSi (OC}_2\text{H}_5)_3} + \text{H}_2\text{O} \rightarrow \underset{\text{(silanol)}}{\text{CH}_2\text{CHSi(OH)}_3} + 3\text{C}_2\text{H}_2\text{OH}$$

$$\text{CH}_2\text{CHSi (OH)}_3 + \text{H}_2\text{O} + \text{Fiber–OH} \rightarrow \text{H}_2\text{CHSi(OH)}_2\text{O–Fiber} + \text{H}_2\text{O}$$

Arrangement

The measurements reported in this article were performed with a TPS element of the type shown in Figure 1. It was made of 10-μm-thick nickel foil with an insulating layer made of 50-μm-thick kapton on each side of the metal pattern. The evaluation of these measurements was performed in the way outlined by Gustafsson.[25] In experiments with insulating layers of such thickness, it is necessary to ignore the voltage

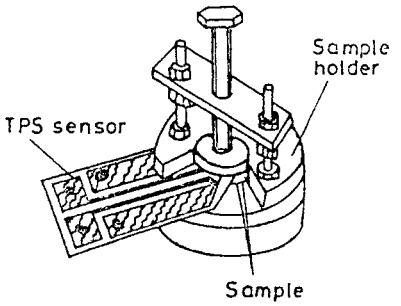

Figure 4 Diagram of the sample holder with the TPS sensor.

recorded during the first few seconds because of the influence of the insulating layers. However, because of the size of the heated area of the TPS element, the characteristic time of such experiments is so long that it is possible to ignore a few seconds of recorded potential difference values and still get very good results.

No influence could be recorded from the electrical connections, which are shown in Figure 2. These connecting leads had the same thickness as the metal pattern of the TPS element. Each TPS element had a resistance at room temperature of about 5.36 Ω and a TCR of around 4.6×10^{-3} K^{-1}.

An important aspect of the design of any TPS element is that as large a part of the hot area as possible should be covered by the electrically conducting pattern, as long as there is insulation between the different parts of the pattern. This is particularly important when insulating layers are covering the conduction pattern and the surface(s) of the sample. It should be noted that the temperature difference across the insulating layer can, after a short initial transient, be considered constant.

The composites were in the form of squares (20 mm $\times$ 20 mm $\times$ 3 mm), and the surfaces of the composites were made smooth to ensure perfect thermal contact between the samples and the heating elements, as the TPS sensor was sandwiched between the two composites of the sample material in the sample holders, as shown in Figure 4. The entire arrangement of the sample holder with the composites was placed in an electric furnace, which was maintained at a constant temperature within ± 1°C. Several runs of the experiments were performed at each recorded temperature to ensure the reproducibility of the results. Also, for thermal equilibrium to be attained, the composites were maintained at a particular temperature for at least 2 h before the experimental data were taken. The change in the voltage was recorded with a digital voltmeter, which was online to the personal computer. The power output to the samples was adjusted according to the nature of the sample material and was, in most cases, in the range of 6×10^{-6} to 16×10^{-6} W/m.[2]

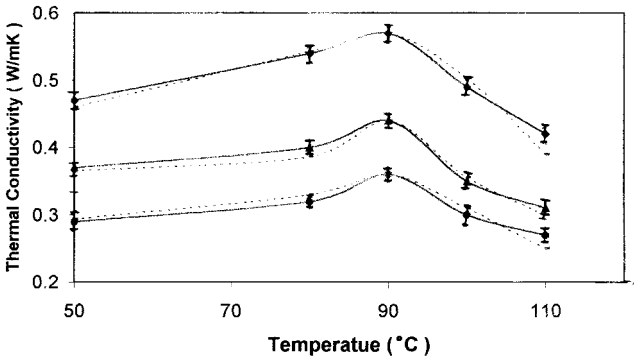

Figure 5 Temperature variation of the thermal conductivity of the composites: (♦) treated with alkali, (▲) treated with silanol, (●) treated with acetic acid, and (–) theoretical.

RESULTS AND DISCUSSION

The values of the thermal conductivity (λ) and thermal diffusivity (χ) of PF were 0.348 W/m K and 0.167 mm^2/s, respectively. The experimental values of λ_e and χ_e of the untreated composites with 40% fiber concentrations were 0.293 W/m K and 0.158 mm^2/s, respectively. The λ_e and χ_e values of the composites treated with alkali, silanol, and acetic acid, measured at 50, 80, 90, 100, and 110°C with the TPS method, are plotted in Figures 5 and 6, respectively, together with the experimental error data with error bars. The alkali-treated composite had higher values of λ_e and χ_e than the other composites. The alkali treatment of the fibers increased the diameter as well as the number of pores on the fiber surface. The increased pore diameter allowed better interlocking with resins and contributed to λ_e and χ_e more than that of the other treated composites. The silane treatment of the fibers made the fibers less hydrophilic and reduced the adhesion between the treated fibers and the hydrophilic phenolic resin. The decrease in the pore diameter due to the treatment weakened the interlocking with the resin, and so λ_e and χ_e were less than those of the alkali-treated composite. The reaction of the acetic acid with

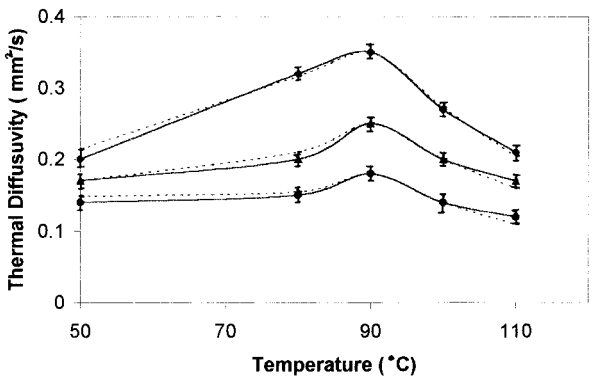

Figure 6 Temperature variation of the thermal diffusivity of the composites: (♦) treated with alkali, (▲) treated with silanol, (●) treated with acetic acid, and (–) theoretical.

the cellulosic OH— groups of the fibers removed the waxy cuticle layer of the fiber surface and increased the polarity of the oil palm fibers. The increase in the polarity reduced the mean free path of the phonons, and so λ_e and χ_e of this composite decreased.

Also, λ_e and χ_e were nonlinear functions of temperature for each composite. A peak was observed at about 90°C for each treated composite. By means of a least-squares fit to the experimental data as a function of temperature (as plotted in Figs. 5 and 6), empirical relationships were developed for the theoretical prediction of λ_e and χ_e:

$$\lambda(T) = A + B(T_0 - T)^2 + D(T_0 - T)^3 \quad (8)$$

$$\chi(T) = a + b(T_o - T)^2 + d(T_0 - T)^3 \quad (9)$$

where A, B, D, a, b, and d are constants, calculated by experimental conditions listed in Tables I and II, that are polymer-dependent. This means that they should change with the different treatments of the composites. T_0 is the temperature at which λ_e and χ_e become maximum, and this temperature lies in the vicinity of the glass-transition temperature in the glass-transition region. T is the temperature of the composite in absolute temperature units.

The observed variations in λ_e and χ_e with temperature can be explained by the effect of the temperature on the structural units in a phenomenological manner.[26–27] In the temperature range below T_0, the temperature dependence of λ_e and χ_e was controlled by the variations of the phonon mean free path due to structural scattering, stray scattering, and chain defect scattering.

For temperatures below T_0, structure scattering became predominant, in addition to chain defect scattering,[28] scattering due to defects introduced by blends and relatively smaller lengths of chain segments. With rising temperatures, the polymeric chain straightened out more and more. Therefore, the mean free path increased,[29] and this resulted in the increases of λ_e and χ_e in this temperature range.

At T_0 (which was very close to the glass-transition temperature of the system), the point at which the crosslinking density of the material became minimum, resulting in a maximum value of the phonon mean free path, λ_e and χ_e became maximum.

TABLE I
Values of the Constants (*A*, *B*, and *D*) in Equation (8) with Different Treatments

Composite	A (W/m K)	$B \times 10^{-4}$ (W/m K^3)	$D \times 10^{-5}$ (W/m K^4)
Alkali-treated	0.25	−4.1	0.9
Silane-treated	0.35	−6.5	1.4
Acetate-treated	0.18	−1.65	0.35

TABLE II
Values of the Constants (*a*, *b*, and *d*) in Equation (9) with Different Treatments

Composite	a (mm^2/s)	$b \times 10^{-4}$ (mm^2/s K^2)	$d \times 10^{-5}$ (mm^2/s K^3)
Alkali-treated	0.57	−6.52	1.47
Silane-treated	0.44	−7.18	1.68
Acetate-treated	0.36	−4.88	1.11

For temperatures above T_0, scattering by microvoids (vacant-site scattering) became predominant, in addition to structure scattering. As the temperature increased and the polymer passed to a rubbery state through a leathery state, gradually individual units, atomic groups, and small-chain segments underwent intensive thermal motions, and the sliding of chain segments started to play a dominant role in governing the variation of the properties with the temperature. This had a twofold effect on the structure of the system; initially, the dominant chain moments created some vacant site or microvoids, which scattered phones in a way similar to that of the point defects.[30] With a rise in the temperature, the number and size of these microvoids increased, and this resulted in a decrease of the mean free path. Therefore, λ_e and χ_e decreased with an increase in the temperature above T_0.

Figures 5 and 6 also show the variations of λ_e and χ_e with temperature as predicted by empirical relations (8) and (9). It is clear from Figures 5 and 6 that the agreement between the predicted values of λ_e and χ_e from the empirical relations and the results of experimentation was very good.

CONCLUSIONS

From the results, it can be concluded that differently treated fiber composites at different temperature give different values of λ_e and χ_e. In the vicinity of the glass-transition temperature, the λ_e and χ_e values of all the composites became maximum because of the creation of more microstructures and, therefore, minimum crosslinking density.

One of the authors (K.S.) is thankful to the Department of Physics at the University of Rajasthan (Jaipur, India) for providing a research scholarship.

References

1. Bhowmik, T.; Pattanayak, S. Cryogenics 1990, 30, 116.
2. Kuzak, S. G.; Hittz, J. A.; Waitkus, P. A. J Appl Polym Sci 1998, 67, 264.
3. Ma, C. C. M.; Tseng, H. T.; Wu, H. D. J Appl Polym Sci 1998, 69, 1119.
4. Jaks, Y.; Jeelan, L.; Rancher, G.; Pearce, E. M. J Appl Polym Sci 1998, 27, 913.

5. Knop, A.; Pilot, L. A. Phenolic Resins; Springer-Verlag: Berlin, 1985; p 162.
6. Rossa, E. P. Plast Eng 1988, 39, 62.
7. Bishop, G. R.; Sheard, P. A. Compos Struct 1992, 21, 85.
8. Ma, C. C. M.; Shih, W. C. U.S. Pat. 4,873,128 (1989).
9. Raj, R. G.; Kokta, B. V.; Groleau, G.; Danneault, C. Plast Rubber Proc 1989, 11, 215.
10. Jyonsik, J.; Hyuksung, C.; Myonghwan, Y. K. J Appl Polym Sci 1988, 69, 2043.
11. Rozman, H. D.; Peng, G. B.; Ishak, M. Z. J Appl Polym Sci 1988, 70, 2647.
12. Sreekala, M. S.; Thomas, S.; Kumaran, M. G. J Appl Polym Sci 1997, 66, 821.
13. Agrawal, R.; Saxena, N. S.; Sharma, K. B.; Sreekala, M. S.; Thomas, S. Indian J Pure Appl Phys 1999, 37, 865.
14. Gustafsson, S. E. Z Naturforsch 1967, 121, 1005.
15. Gustafsson, S. E.; Kawasaki, E.; Khan, M. N. J Phys D: Appl Phys 1979, 121, 1411.
16. Saxena, N. S.; Chohan, M. A.; Gustafsson, S. E. J Phys D: Appl Phys 1986, 10, 1625.
17. Bala, K.; Pradhan, P. R.; Saxena, N. S.; Saksena, M. P. J Phys D: Appl Phys 1989, 22, 1068.
18. Gustafsson, S. E.; Kawasaki, E. Rev Sci Instrum 1983, 54, 744.
19. Gustafsson, S. E.; Kawasaki, E.; Khan, M. N. J Appl Phys 1979, 52, 2596.
20. Pradhan, P. R.; Sachdev, K.; Bala, K.; Saxena, N. S.; Saksena, M. P. Int J Energy Res 1991, 15, 49.
21. Haq, I. U.; Saxena, N. S.; Gustafsson, S. E.; Maqsood, A. Heat Recovery CHP 1991, 11, 299.
22. Singh, K.; Saxena, N. S.; Maharjan, N. B. Phys Status Solidi A 2002, 189, 197.
23. Dashora, P.; Saxena, N. S.; Saksena, M. P.; Bala, K.; Sachdev, K.; Pradhan, P. R.; Ladiwala, G. D. Phys Scripta 1992, 45, 399.
24. Agrawal, R.; Saxena, N. S.; Sreekala, M. S.; Thomas, S. J Appl Polym Sci 2000, 38, 916.
25. Gustafsson, S. E. Rev Sci Instrum 1991, 62, 797.
26. Gustafsson, S. E.; Suleiman, B.; Saxena, N. S.; Haq, I. U. High Temp High Pressure 1991, 23, 284.
27. Dashora, P. Phys Scripta 1994, 46, 611.
28. Peepechoko, I. I. An Introduction to Polymer Physics; Mir: Moscow, 1981.
29. Saxena, N. S.; Pradeep, P.; Mathew, G.; Thomas, S.; Gustafsson, M.; Gustafsson, S. E. Eur Polym J 1999, 35, 1687.
30. Lee, T. C. P.; Millens, W. (to Gould, Inc.). U.S. Pat. 8,344,044 (1977).